Available online at www.sciencedirect.com
SCIENCE DIRECT®
PERGAMON
International Journal of Heat and Mass Transfer 46 (2003) 4427–4438
International Journal of HEAT and MASS TRANSFER
www.elsevier.com/locate/ijhmt

Natural convection heat transfer of microemulsion phase-change-material slurry in rectangular cavities heated from below and cooled from above

H. Inaba [a,*], C. Dai [b], A. Horibe [a]

[a] Department of Mechanical Engineering, Faculty of Engineering, Okayama University, Tsushimanaka 3-11, Okayama 700-8530, Japan
[b] Graduate School of Natural Science and Technology, Okayama University, Okayama 700-8530, Japan

Received 10 May 2002; received in revised form 1 May 2003

Abstract

An experimental study has been conducted in dealing with natural convection heat transfer characteristics of microemulsion slurry in rectangular enclosures. The microemulsion slurry used in the present experiment was composed of water, surfactant, and fine particles of phase-change-material (PCM). The PCM mass concentration of the microemulsion slurry was varied from a maximum 30 mass% to a diluted minimum 5 mass%, and the experiments have been done separately in three subdivided temperature ranges of the dispersed PCM particles in a solid phase, two phases (coexistence of solid and liquid) and a liquid phase. The results showed that the Nusselt number increased slightly with the PCM mass concentration for the slurry in solid phase. In the phase change temperature range, the Nusselt number increased with an increase in PCM mass concentration of the slurry at low Rayleigh numbers, while it decreased with increasing PCM mass concentration of the slurry at high Rayleigh numbers. There was not much difference in natural heat transfer characteristics of the PCM slurry with low PCM concentrations (<10 mass%), however, the difference was getting greater with increasing the PCM concentration, especially for the enclosure at a lower aspect ratio (width/height of the rectangular enclosure). The enclosure height was varied from 5.5 to 24.6 mm under a fixed width and depth of 120 mm. Hence, the experiments were performed for a wide range of modified Rayleigh number from 3×10^2 to 1.0×10^7. The correlation generalized for the PCM slurry in a single phase was derived in the form of $Nu = 0.22(1 - C_1C_m e^{-C_2AR})Ra^{1/(3n+1)}$, where C_1 and C_2 were the optimum fitting constants obtained by the least square method. While the PCM was in a phase changing region, the correlation could be expressed as $Nu = 0.22(1 - C_1C_m e^{-C_2AR})Ra^{1/(3n+1)}Ste^{-0.25}$, where the *Ste* was the modified Stefan number.

1. Introduction

The exploitation of functionally thermal fluid has been giving an increasing attention in recent years for their great potentials to be utilized in heat transfer, heat storage and fluid transportation [1,2]. The practical feasibility studies had already been done by numerous researchers for the forced convection using the microencapsulated phase change material slurry [3–5]. However, there are very few investigations on the natural convection heat transfer characteristics for the PCM slurry. The main problem, which has to be overcome, is the effect of stratification and/or agglomeration due to a large size of particle for the natural convection in the PCM slurry. However, the present technique could produce the fine encapsulated particles of the PCM in a diameter of less than one micrometer, which is much smaller than those used by Datta et al. [6] and Katz [7]. Recently, the experimental study conducted by Datta et al. [8] showed that the PCM slurry at low concentration (<5%) could enhance the heat transfer in natural convection in a couple of their experiments. The effects on the natural convection heat transfer characteristics for a

* Corresponding author. Tel.: +81-86-251-8046; fax: +81-86-251-8266.
E-mail address: inaba@mech.okayama-u.ac.jp (H. Inaba).

0017-9310/$ - see front matter © 2003 Elsevier Ltd. All rights reserved.
doi:10.1016/S0017-9310(03)00289-8

Nomenclature

a	thermal diffusivity ($m^2\,s^{-1}$)
AR	aspect ratio, width/height of rectangular enclosure
C_1	coefficient in correlation
C_2	coefficient in correlation
C_m	mass concentration
C_p	apparent specific heat ($J\,kg^{-1}\,K^{-1}$)
D	depth of rectangular enclosure (mm)
d	particle diameter (μm)
g	gravitational acceleration ($m\,s^{-2}$)
H	height of rectangular enclosure (mm)
k	thermal conductivity ($W\,m^{-1}\,K^{-1}$)
K	consistency index of power law model fluid ($Pa\,s^n$)
m	mass (kg)
n	pseudoplastic index of power law model fluid
Nu	Nusselt number, Eq. (9)
Pr	Prandtl number
q	net heat flux through the water or PCM slurry layer ($W\,m^{-2}$)
q_t	gross electric power input ($W\,m^{-2}$)
Ra	Rayleigh number, Eq. (10)
Ste	Stefan number, Eq. (12)
T	temperature (K)
W	width of rectangular enclosure (mm)
x	mass ratio, m_{30}/m_w
Y	dimensionless vertical coordinate

Greek symbols

α	heat transfer coefficient, $q/(T_H - T_C)$ ($W\,m^{-2}\,K^{-1}$)
β	volumetric expansion coefficient (K^{-1})
γ	strain rate (s^{-1})
ρ	density ($kg\,m^{-3}$)
v	kinematic viscosity ($m^2\,s^{-1}$)

Subscripts

H	heating plate
C	cooling plate
0	reference state
cal	calculated from the correlating equation
exp	experimental
r	room
s	solid phase
w	water
30	PCM mass concentration of 30%

wide range of the PCM mass concentration of the slurry and various aspect ratios of the rectangular enclosure have been investigated in the present study.

2. The properties of microemulsion PCM slurries

The original microemulsion PCM slurry was a mixture of paraffin, surfactant, and water in a mass ratio of 30%, 5%, and 65%, respectively. The external appearance is shown in Fig. 1. The polymer surfactant composed of hydrophilic radicals in the water side and hydrophobic radicals in the paraffin (oil) side acts as an emulsifier or a thin film separating the PCM from water. The PCM particles and water are immiscible each other. The stability and fluidity of the PCM particles can be achieved due to the thin films (2–5 nm in thickness) of the polymer surfactant around them. The polymer surfactant keeps fluidity, and is stable while the PCM is under a phase change. The thermal resistance of the polymer surfactant can be negligible. It is considered that while the PCM inside the particles is in a liquid phase, the internal circulation of the PCM occurs and the polymer surfactant film is movable. However, while the PCM is in a solid phase, there is no internal circulation of the PCM. As a result, the drag coefficient by natural convection is lower for the PCM in the liquid phase than that for the PCM in the solid phase [2].

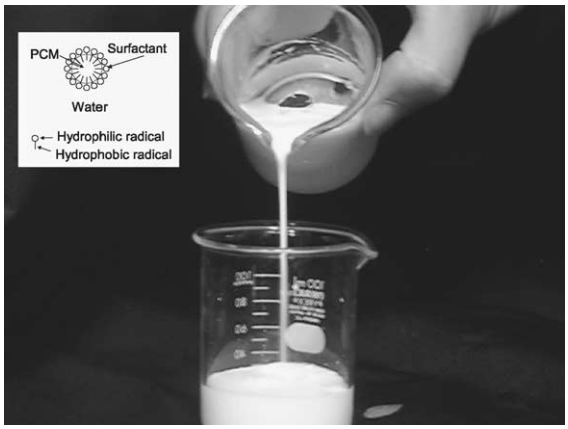

Fig. 1. The external appearance of microemulsion slurry ($C_m = 30\%$).

By diluting the original microemulsion PCM slurry ($C_m = 30\%$) with distilled water, the less concentrated PCM slurries could be made. As shown in Fig. 2, the PCM particle diameter distribution ranged from 0.1 to 1.2 μm and its volumetric averaged diameter was $d_m = 0.51$ μm. A 200 ml separatory funnel was used to check if any stratification occurs for the original PCM slurry. The density distributions of the original and the heated PCM slurry (up to 328 K) were inspected. The

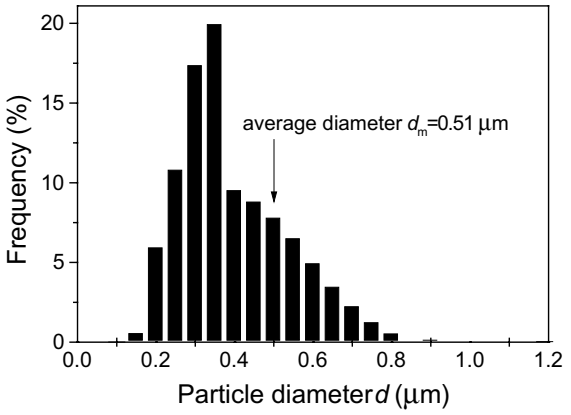

Fig. 2. The PCM particle size distribution.

results showed no evidences of any stratification of the PCM particles in the slurry. The apparent specific heat C_p was measured using a differential scanning calorimeter (DSC). The data obtained by using water were in agreement with the reference values [9] with a standard deviation of ±1.5%. The measured data of apparent specific heat of the PCM slurry with a PCM mass concentration of 30% were plotted against temperature in Fig. 3. The pycnometer was used for measuring the density, which had a measuring accuracy of within $\pm 5.0\times10^{-4}$ kg m^{-3}. The thermal conductivity was measured by the present experimental apparatus under the conditions of top wall heating and bottom wall cooling, and its measuring method will be described in the later section. The viscosity parameters for various PCM concentrations of the slurry as shown in Fig. 4 were measured using a rotary cylinder viscosity meter. The measured viscosities for water were in agreement with reference values [9] with a standard deviation of ±1.2% in the temperature range from 303 to 333 K. Fig. 5a and

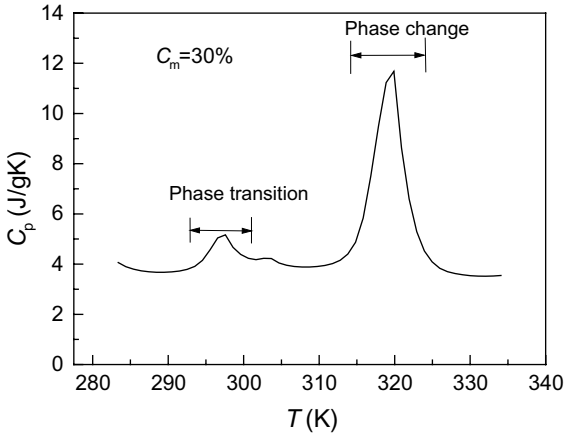

Fig. 3. Apparent specific heat capacity measured by DSC.

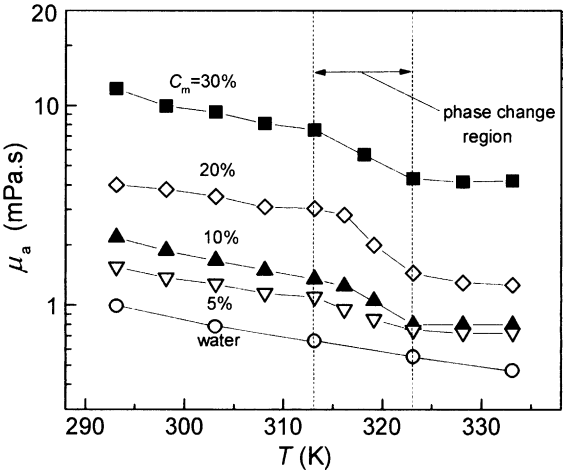

Fig. 4. The relationship of apparent viscosity with temperature for various concentration microemulsion slurries at strain rate of $\gamma = 14.5$ s^{-1}.

b show the measured pseudoplastic fluid index n and viscosity consistency K against temperature T, respectively. At a same strain rate, the viscosity is higher for the PCM in a solid phase than that for the PCM in a liquid phase. In other words, the microemulsion PCM slurry gets less viscid with the melting of the PCM particles in slurry. The more diluted or the less concentrated PCM slurry also becomes less viscid. Fig. 6 shows the relationship between the volumetric expansion coefficient β and temperature T for the PCM slurry. The volumetric expansion coefficient was measured using a volumetric expansion meter. The measured data of water were in agreement with reference values [9] with a standard deviation of less than ±1%. It is shown in Fig. 6 that the volumetric expansion coefficient increases with an increase in temperature from $T = 310$ K, and it reaches a maximum one at a temperature of about 319 K. The data of β show that the local maximum volumetric expansion coefficient decreases with a decrease in the PCM mass concentration C_m of the slurry. As can be seen in Fig. 3 or Fig. 4, the phase changing region of the PCM almost covers the temperature range from 313 to 323 K. Hence, the temperature range in the experiments was intentionally divided into three subregions according to the phase of PCM particles, which were the solid region ($T < 313$ K), the phase changing region (313 K $< T <$ 323 K) and the liquid region ($T >$ 323 K). The density ρ, the thermal conductivity k, the volumetric expansion coefficient β, and the apparent specific heat C_p for the diluted microemulsion PCM slurries can be calculated by using Eqs. (1)–(4), which were derived by the proportional relation between the measured properties of the 30 mass% microemulsion PCM slurry and those of water. Where x is the mass ratio of water to the PCM slurry (30 mass%). As it is well known that the natural

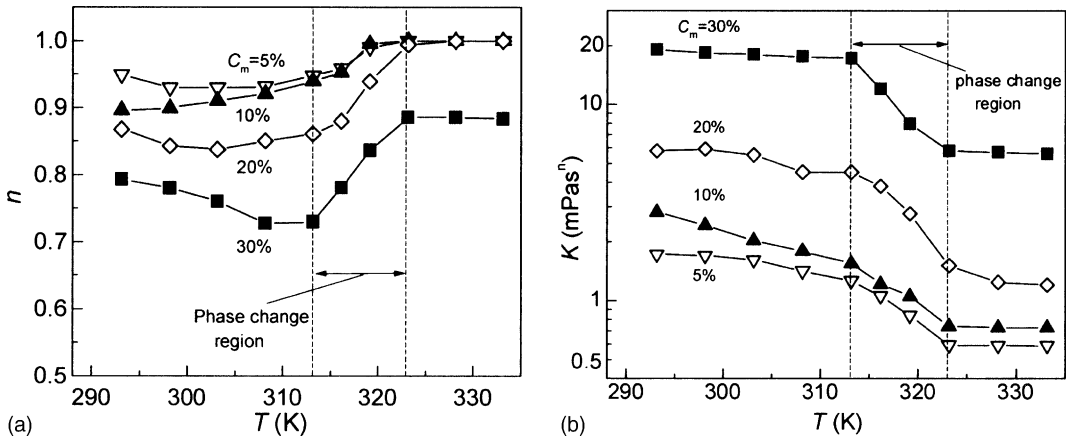

Fig. 5. The variations of pseudoplastic fluid index n (a), and viscosity consistency K (b) with temperature at various concentrations of microemulsion slurry.

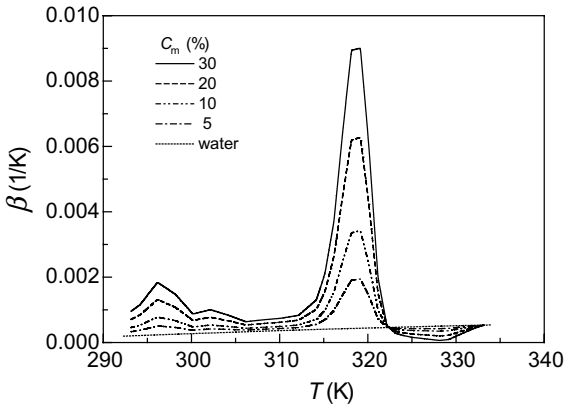

Fig. 6. The relationship between volumetric expansion coefficient β and temperature at various mass concentrations of microemulsion slurry.

$$k_{\mathrm{mix}} = \left(k_{\mathrm{w}} + k_{30}\frac{\rho_{\mathrm{w}}}{x\rho_{30}}\right)\Big/\left(1+\frac{\rho_{\mathrm{w}}}{x\rho_{30}}\right) \tag{3}$$

$$C_{p\mathrm{mix}} = \left(C_{p\mathrm{w}} + \frac{C_{p30}}{x}\right)\Big/\left(1+\frac{1}{x}\right) \tag{4}$$

The measured density ρ_{30}, volumetric expansion coefficient β_{30}, apparent specific heat C_{p30}, and thermal conductivity k_{30} for the microemulsion PCM slurry with a PCM mass concentration of 30% can be expressed, respectively, in the following equations.

$$\rho_{30} = \begin{cases} 1181. - 0.7162T & 303\ \mathrm{K} \leqslant T < 313\ \mathrm{K} \\ 916.8 + 39.57/\left(1+\mathrm{e}^{\frac{T-318.5}{1.19}}\right) & 313\ \mathrm{K} \leqslant T \leqslant 323\ \mathrm{K} \\ 1267. - 1.08T & 323\ \mathrm{K} < T \leqslant 333\ \mathrm{K} \end{cases} \tag{5}$$

$$\beta_{30} = \begin{cases} 1.11 - 7.19\times10^{-3}T + 1.17\times10^{-5}T^2 & 303\ \mathrm{K} \leqslant T < 313\ \mathrm{K} \\ 7.14\times10^{-4} + 0.00845\mathrm{e}^{-0.2(T-318.5)^2} & 313\ \mathrm{K} \leqslant T \leqslant 323\ \mathrm{K} \\ 1.49 - 9.09\times10^{-3}T + 1.39\times10^{-5}T^2 & 323\ \mathrm{K} < T \leqslant 333\ \mathrm{K} \end{cases} \tag{6}$$

convection is a non-linear dissipative dynamic system essentially coupled between flow and heat transport. Much more complicated natural convection characteristics are to be expected with these complicated physical properties.

$$\rho_{\mathrm{mix}} = \rho_{30}\left(1+\frac{1}{x}\right)\Big/\left(\frac{\rho_{30}}{\rho_{\mathrm{w}}}+\frac{1}{x}\right) \tag{1}$$

$$\beta_{\mathrm{mix}} = \left(\beta_{\mathrm{w}} + \beta_{30}\frac{\beta_{\mathrm{w}}}{x\rho_{30}}\right)\Big/\left(1+\frac{\rho_{\mathrm{w}}}{x\rho_{30}}\right) \tag{2}$$

$$k_{30} = \begin{cases} 0.268 + 7.07\times10^{-4}T & 303\ \mathrm{K} \leqslant T < 313\ \mathrm{K} \\ 2.929 - 0.00776T & 313\ \mathrm{K} \leqslant T \leqslant 323\ \mathrm{K} \\ -0.279 + 0.00212T & 323\ \mathrm{K} < T \leqslant 333\ \mathrm{K} \end{cases} \tag{7}$$

$$C_{p30} = \begin{cases} 1559. - 10.09T + 0.01636T^2 & 303\ \mathrm{K} \leqslant T < 313\ \mathrm{K} \\ 4.464 + 7.134\mathrm{e}^{-0.162(T-319.2)^2} & 313\ \mathrm{K} \leqslant T \leqslant 323\ \mathrm{K} \\ 3.51 + 1.013\mathrm{e}^{-0.551(T-323.9)} & 323\ \mathrm{K} < T \leqslant 333\ \mathrm{K} \end{cases} \tag{8}$$

3. Experimental setup and procedures

The schematic diagram of experimental setup is shown in Fig. 7. The cut view of the test section is shown in Fig. 8. The rectangular enclosure consisted of a transparent acrylic side-frame (10 mm thick) and two copper plates (10 mm thick). The copper plates were fitted to the top and bottom ends of the side-frame. The temperature of the top cooling copper plate was maintained at a constant by circulating the cooling brine through the backside of the cooling copper plate. A 0.7 mm thick electric film heater was mounted below the bottom of the lower copper heating plate. A film heat flux sensor (0.2 mm thick and 50 mm in square), which had a measuring accuracy of 1.0 $W m^{-2}$, was inserted between the film heater and the lower copper heating plate. The backside of the film heater was covered with a 5 mm thick foamed thermal insulating material, and a 15 mm thick bakelite plate was mounted below the thermal insulating material. The whole test section was thermally insulated by a 50 mm thick foamed thermal insulating material. A glass pipe of 8.0 mm in an inner diameter was designed as an expansion reservoir of the microemulsion slurry. The average temperatures of the heating and cooling copper plates were measured, respectively, by six 0.1 mm diameter Cu–Co thermocouples, and two of the six thermocouples were buried in the middle and four of them were located around of the heating or the cooling plate. All the thermocouples had been individually calibrated in a constant-temperature water bath to yield a measuring precision of ±0.2 K. The temperature of the heating copper plate was adjusted by controlling the electric power input of the heater. The height of the rectangular enclosure H or the aspect ratio AR can be changed easily by selecting a suitable acrylic side-frame with a different height. Two T-type thermocouples supported by a 1.06 mm in an outer diameter and 0.18 mm thick stainless pipe were installed to measure the vertical temperature distribution in the center of the enclosure, and, their positions in the vertical y-direction were controlled with a micrometer.

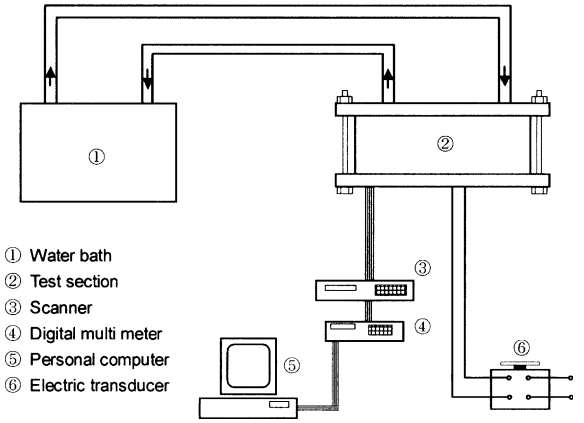

Fig. 7. Schematic diagram of experimental apparatus.

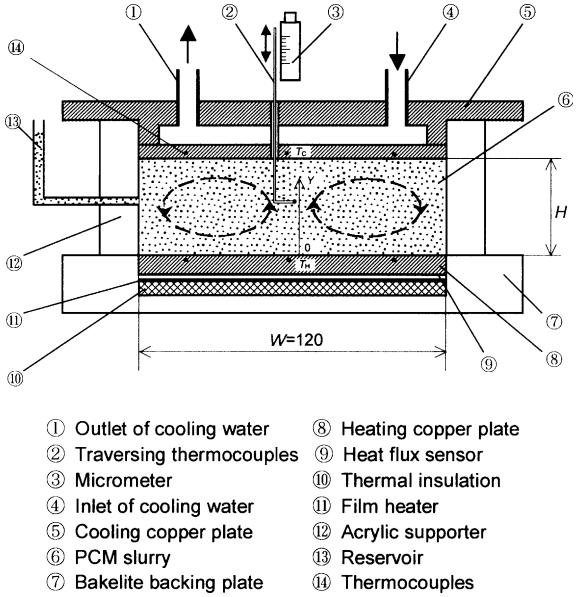

Fig. 8. Cut view of test section.

In order to estimate the heat-loss from the experimental apparatus to the environment, firstly, the apparatus was calibrated under the heat conduction condition of the top wall heating and the bottom wall cooling by using distilled water. Then the heat-loss can be estimated by withdrawing the net heat based on heat conduction through the water layer from the gross electric power input of the film heater. The experiments were repeated with different electric power inputs and temperature differences between the heating copper plate and the environment. The results showed that the heat-loss was approximately a linear function of the temperature difference between the heating copper plate and the environment. The heat-loss from the experimental apparatus was less than 5% of the total heat input. The measured thermal conductivities of the distilled water by using the calibrated experimental apparatus were in agreement with the reference values [9] with a standard deviation of ±2%. The thermal conductivity of the microemulsion slurry was measured by using the same experimental apparatus. The measured Nu number against Ra number for the distilled water and the rectangular enclosure of $H = 8.4$ mm (AR = 14.3) was approximately 4.5% lower than that calculated by using Holland's equation [10] due to the side-wall effect, since this equation applied to the natural convection between two infinite plates. Therefore, it was clear that the precision of the present experimental apparatus was enough

to estimate the natural convection heat transfer of the PCM slurry layer.

The top cooling plate temperature was fixed at 303, 313 and 323 K for the PCM in solid phase, phase changing and liquid phase regions, respectively. Data acquisition was conducted while the whole system was considered at a thermal steady state if the heating plate had a temperature fluctuation within ±0.05 K in an hour. In addition, the averaged heating plate temperature T_H, the electric power input q_t, the room temperature T_r and the PCM slurry temperature T_f at the center of the enclosure were monitored with time from the beginning to the end of the experiment in every 30 s. The uncertainties in the measured Rayleigh number and Nusselt number were estimated to be 7% and 6%, respectively.

4. Experimental results and discussion

4.1. The PCM in solid phase

In relation to the non-dimensionalization of experimental data, the buoyancy induced natural convection heat transfer around a vertical plate can be generally expressed as a function of Rayleigh number *Ra* and Prandtl number *Pr* under an either isothermal or constant heat flux heated condition [11]. For the natural convection heat transfer in a rectangular enclosure, the aspect ratio of the enclosure should be included to account the side-wall effect [12]. In fact, the side-wall of an enclosure plays a significant role in a convective-flow structure analysis [13]. However, the natural convection in a non-Newtonian fluid becomes much more complicated. The reason is that the viscosity of a non-Newtonian fluid is dependent on stress or strain rate. For the shear-thinning pseudoplastic non-Newtonian fluid, the definition of Rayleigh number can be obtained easily by a standard normalization of N–S equation if the velocity scale is given by a_0/H, pressure scale by $\rho_0 a_0^2/H^2$, and time scale by H^2/a_0 [14]. The experimental results of the natural convection heat transfer can be generalized by *Nu* number against *Ra* number, where Nusselt number *Nu* and Rayleigh number *Ra* were defined, respectively, as follows:

$$Nu = \frac{\alpha H}{k} \tag{9}$$

$$Ra = \frac{\rho_0 g \bar{\beta}(T_H - T_C) H^{2n+1}}{K a_0^n} \tag{10}$$

The heat transfer coefficient α is defined as $\alpha = q/(T_H - T_C)$, where q is the net heat flux through the PCM slurry or water layer. The volumetric expansion coefficient $\bar{\beta}$ was an integral averaged value from the temperature of top cooling plate to the temperature of bottom heating plate. Up to now, it is still difficult for getting a generalized dependency to evaluate the natural convection in a non-Newtonian fluid [15–17].

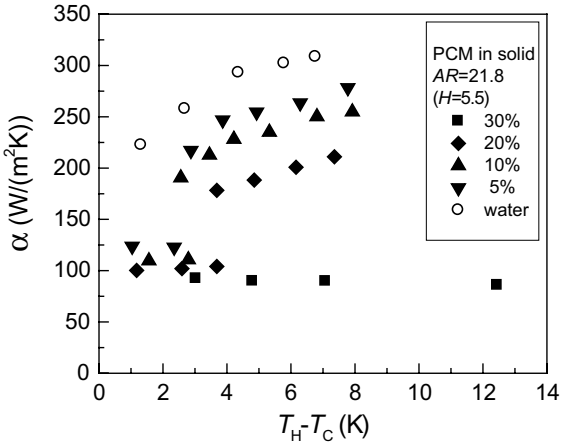

Fig. 9. The heat transfer coefficient versus the temperature difference between the two horizontal boundaries for the PCM slurries with various mass concentrations for AR = 21.8 ($H = 5.5$ mm) and the PCM in solid phase.

Fig. 9 shows the heat transfer coefficient α versus the temperature difference $T_H - T_C$ ($T_C = 303$ K) between two horizontal boundaries for various PCM mass concentrations of the slurries in the case of AR = 21.8 or $H = 5.5$ mm and for the PCM in solid phase. It is shown that no convection occurred for the highest PCM mass concentration of 30 mass%, and the heat transfer coefficients keep almost constant. For the slurry with a lower PCM mass concentration, a convection state can be induced with an increase in temperature difference. However, a jump in heat transfer coefficient has been observed from the stable conduction state to the convection state. This means that the subcritical regime exists for the natural convection in the microemulsion slurry. Depending on the initial condition, either a natural convection or a heat conduction state can exist in the subcritical regime. The previous studies showed that the discontinuity of Nusselt number with respect to Rayleigh number at the critical condition resulted mainly from the departure of a real fluid from the Boussinesq approximation [13]. Fig. 9 also shows that the temperature difference required for the jump in heat transfer coefficient from the heat conduction state decreases with a decrease in PCM mass concentration. This phenomenon was also getting disappeared with an increase in enclosure height for the slurry at a PCM mass concentration of 20%, as shown in Fig. 10. Fig. 11 shows the vertical temperature distribution profile in the middle of the enclosure for $C_m = 20\%$, AR = 21.8 and the PCM in a solid phase. The linear temperature distributions, which indicate the steady state of heat conduction at lower heat fluxes, are shown clearly in Fig. 11.

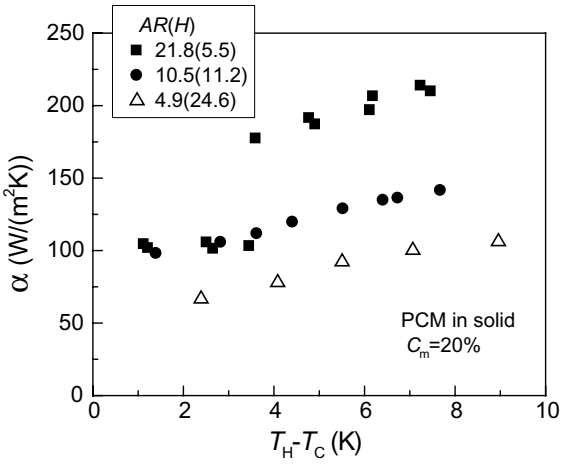

Fig. 10. The heat transfer coefficient versus the temperature difference between the two horizontal boundaries at various aspect ratios for the PCM in solid phase and $C_m = 20\%$.

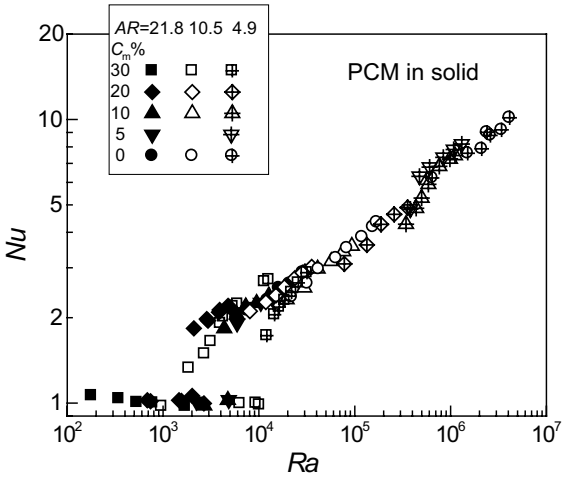

Fig. 12. Nusselt number against Rayleigh number for the PCM in solid phase at various mass concentrations and aspect ratios.

Fig. 12 shows the Nusselt number against Rayleigh number for all the measured data while the PCM in the slurry was in a solid phase for various aspect ratios and PCM mass concentrations. If the experimental results were correlated in the form of equation $Nu = C_s Ra^{1/(3n+1)}$ for each rectangular enclosure and the PCM slurry, the best fitting constant C_s in the equation could be obtained. The exponent of Rayleigh number was taken from the result of natural convection in non-Newtonian fluid around a heated vertical plate [18,19]. As shown in Fig. 13, the fitting constant C_s increases with an increase in aspect ratio AR and a decrease in PCM mass concentration C_m. This indicates that the side-wall effect on heat transfer is reduced with an increase in aspect ratio AR. However, the side-wall effect can be different for various fluids. For the PCM slurry with a PCM mass concentration of 30%, the fitting constant C_s decreases remarkably with a decrease in aspect ratio AR, or, a significant influence of aspect ratio on the Nusselt number has been observed. For pure water, the fitting constant C_s was almost constant in the range of aspect ratio AR = 4.9–21.8. Since the PCM slurry used in the present study is a non-Newtonian fluid, for the enclosures with the same aspect ratio AR, the side-wall effect might be different for power-law non-Newtonian fluids with various n. For instance, the Prandtl number of a power-law

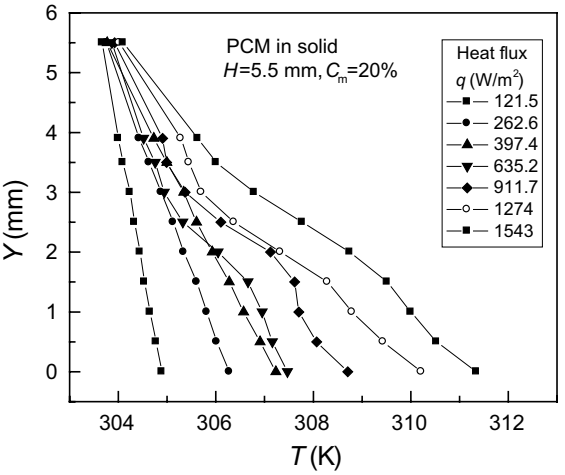

Fig. 11. The vertical temperature distribution in the middle of enclosure for $C_m = 20\%$, AR = 21.8 and the PCM in solid phase.

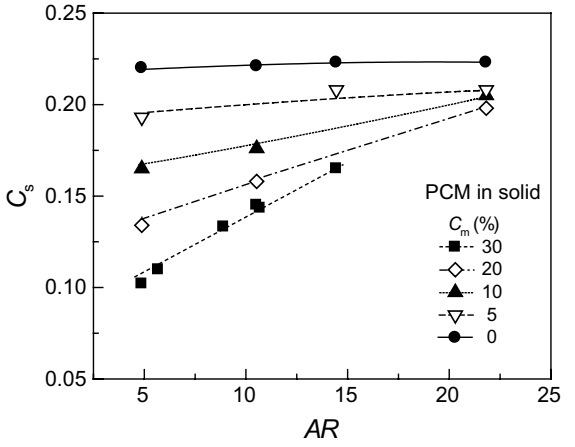

Fig. 13. The best multipliers obtained for fitting the Nusselt numbers against the Rayleigh numbers with a power index of $1/(3n + 1)$ for various aspect ratios and mass concentrations.

fluid can be expressed as $Pr = (Ka_0^{n-2}/\rho_0 H^{2n-2})$ [14], which is related to both H (or AR if W is fixed) and n. In the present experimental correlations, the aspect ratio AR rather than the Prandtl number Pr was considered, because the Prandtl number Pr is also a function of the aspect ratio AR (if W is fixed) for power-law non-Newtonian fluids. Therefore, the correlation of experimental data with the form of $Nu = C_s(1 - AC_m e^{-BAR})Ra^{1/(3n+1)}$ was proposed, which was expected to correlate the data well. Where "A" and "B" in the equation above are the constants to be determined by the least square approximation according to the data shown in Fig. 13. The correlation equation indicates that the Nusselt number decreases with an increase in PCM mass concentration C_m and a decrease in aspect ratio AR. The optimum fitting correlation for the PCM in solid phase is following.

$$Nu = 0.22(1 - 2.7C_m e^{-0.063AR})Ra^{1/(3n+1)} \quad (11)$$

The comparison of Nusselt number between the experimental data and the correlation equation (11) is shown in Fig. 14. The correlation equation (11) is in agreement with the experimental data with a standard deviation of ±4.2%. Here, the applicable parameter ranges in Eq. (11) are $Ra = 1.0 \times 10^3$–6.0×10^6, $C_m = 0$–30%, and AR = 5.0–22.0.

4.2. The PCM in phase changing

As shown in Fig. 5, the microemulsion PCM slurry has very complex thermophysical and rheological properties within the phase changing temperature range from 313 to 323 K. The volumetric expansion coefficient β shows a peak value at a temperature of 319 K. In fact, the PCM used in the present experiment is composed of some kinds of n-paraffin (C_nH_{2n+2}), and the melting point of n-paraffin rises with the molecular number of carbon. For instance, the docosane ($C_{22}H_{46}$) has a melting point of 317.5 K, the tricosane ($C_{23}H_{48}$) of 320.8 K, and, the tetracosane ($C_{24}H_{50}$) of 324.3 K. Fig. 15 shows the convection heat transfer coefficient α versus the temperature difference $T_H - T_C$ ($T_C = 313$ K) between the heating and cooling plates for various PCM mass concentrations in the enclosure of AR = 21.8 ($H = 5.5$ mm). As shown in Fig. 15, a local maximum heat transfer coefficient α appears at the heating plate temperature of $T_H = 319$ K (temperature difference $T_H - T_C = 6$ K). It corresponds to the melting temperature showing the local maximum apparent specific heat as shown in Fig. 3. It was believed that the maximum heat transfer coefficient was mainly due to the participation of the phase changing process of PCM particles in the natural convection heat transfer of the slurry. Fig. 16(a) and (b) show the vertical temperature distribution profiles in the middle of enclosure for the case of $C_m = 20\%$, AR = 21.8 ($H = 5.5$ mm) and the case of $C_m = 30\%$, AR = 10.5 ($H = 11.4$ mm), respectively. The jump in heating plate temperature T_H at $y = 0$ mm in the temperature range of $T > 320$ K was observed in both Fig. 16a and b. This result was attributed to the dramatic decrease in the heat transfer coefficient from temperature difference $T_H - T_C = 6$ K to $T_H - T_C = 10$ K as shown in Fig. 15, since the latent heat transferred during the phase changing process decreased with an increase in heating plate temperature T_H over $T_H = 320$ K.

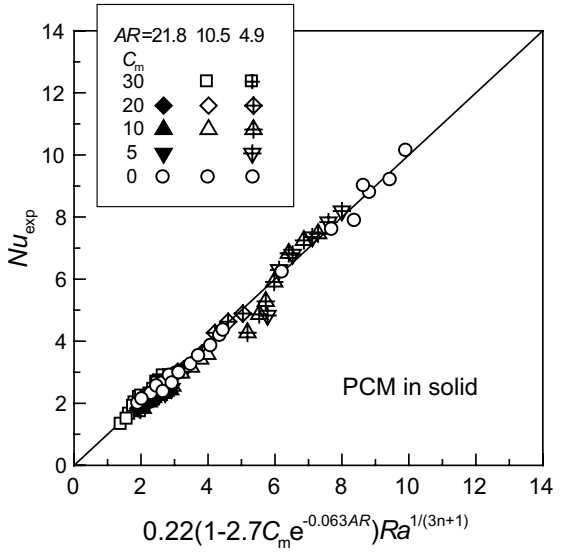

Fig. 14. Comparison of Nusselt number between experimental data and the correlation Eq. (11) for the PCM in solid phase.

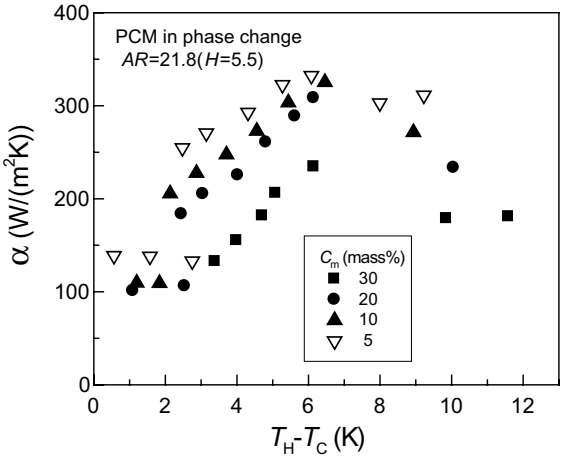

Fig. 15. The heat transfer coefficient versus the temperature difference between the heating and cooling plates for various mass concentration PCM slurries in the enclosure of AR = 21.8 ($H = 5.5$ mm) and for the PCM in phase changing.

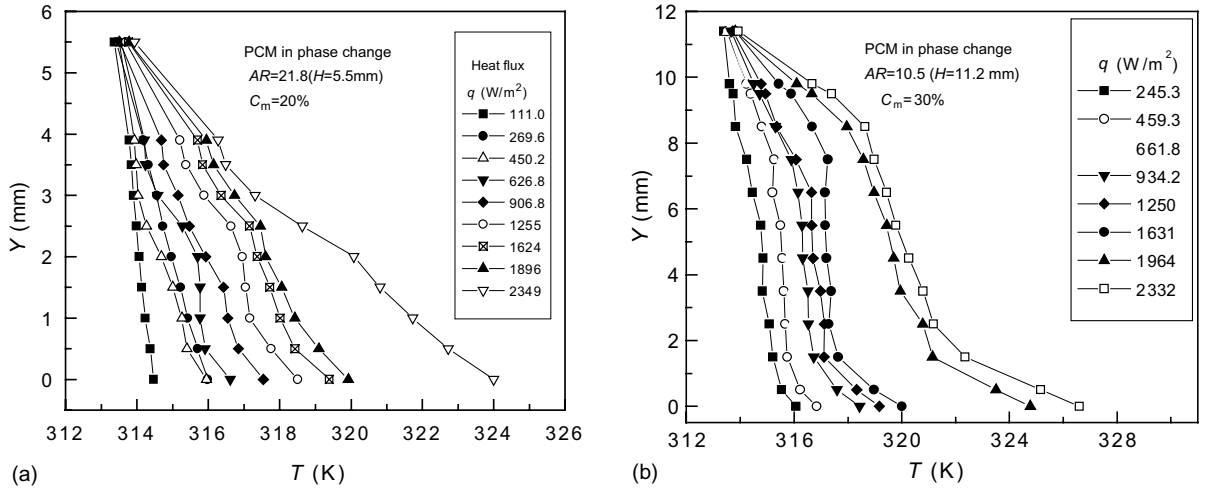

Fig. 16. The vertical temperature distribution profiles in the middle of enclosure for the PCM in phase changing and for the case of $C_m = 20\%$, AR = 21.8 ($H = 5.5$ mm) and the case of $C_m = 30\%$, AR = 10.5 ($H = 11.4$ mm).

Fig. 17 shows the Nusselt number versus Rayleigh number for various aspect ratios AR and PCM mass concentrations C_m. As shown in Fig. 17, even for the PCM slurry with the lowest PCM mass concentration of $C_m = 5\%$, the phenomenon of a rapid decrease in Nusselt number is shown clearly, which corresponds to a jump in bottom heating plate temperature. However, the Nusselt number increases again with an increase in Rayleigh number over $Ra > 2 \times 10^4$, as shown in Fig. 18.

The heat transfer enhancement of natural convection in the PCM microemulsion slurries was considered mainly due to the melting and solidification of the PCM near the heating and cooling boundaries, respectively. Its enhancement should be dependent upon the latent heat or the enthalpy of the PCM slurry in a phase change confined by the two boundary temperatures. The previous numerical results [20] also showed that the latent heat transfer in a phase changing process resulted in the enhancement of natural convection heat transfer between the heating and cooling boundaries. Therefore, the Nusselt number can be correlated with the following modified Stefan number *Ste*.

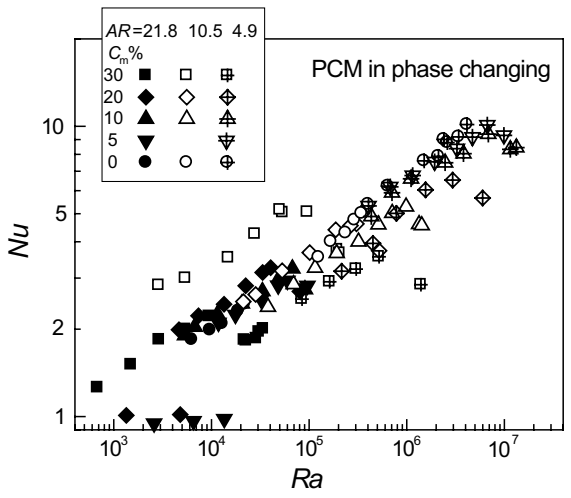

Fig. 17. Nusselt number against Rayleigh number for the PCM in phase changing at various mass concentrations and enclosures.

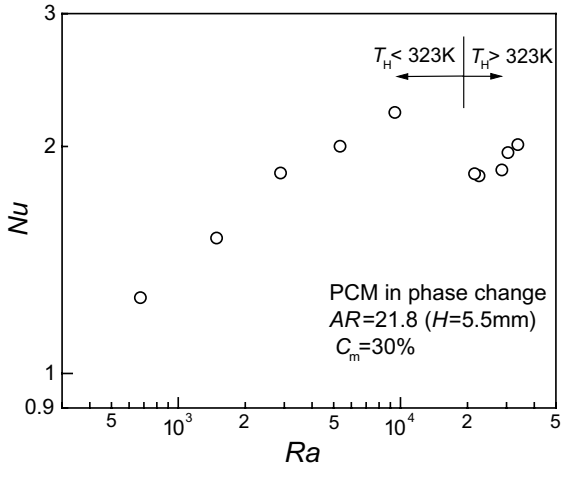

Fig. 18. Nusselt number against the Rayleigh number for $C_m = 30\%$ and AR = 21.8 (The *Nu* number restores increasing again with *Ra* when the heating plate temperature is over the maximum phase changing temperature).

$$Ste = \frac{C_{p0}(T_h - T_c)}{\int_{T_c}^{T_h} C_p \, dT} \tag{12}$$

where C_{p0} is an apparent reference specific heat at 313 K. Note that the apparent specific heat C_p is significantly dependent upon temperature indicated in Fig. 3. Fig. 19 shows the reciprocal of Stefan number versus temperature for various PCM concentrations of the slurry. As it is shown in the figure, the reciprocal of Stefan number increases with an increase in the PCM mass concentration C_m.

The Nusselt number and the Rayleigh number were correlated in the same method described in the above section. However, since the Rayleigh number alone cannot reflect the peak appearance of Nusselt number, the Stefan number defined above was introduced in the correlation. In other words, the contribution of a phase changing process to natural convection heat transfer has to be taken into account. Fig. 20 shows a close relationship between the Nusselt number and the reciprocal of Stefan number obtained for the case of $C_m = 10\%$ and AR = 10.5 ($H = 11.4$ mm). If the other parameters were included and the same equation form as Eq. (11) was used, it was found that the Nusselt number was in proportion to the Stefan number with an approximately exponent of −1/4. The correlation obtained was in the following.

$$Nu = 0.22(1 - 2.7C_m e^{-0.025AR}) Ra^{1/(3n+1)} Ste^{-(1/4)} \tag{13}$$

The standard deviation of the correlation equation (13) was within ±12% against the experimental data, as shown in Fig. 21. The applicable parameter ranges in Eq. (13) are $Ra = 5.0 \times 10^2$–2.0×10^7, $C_m = 0$–30% and AR = 5.0–22.0.

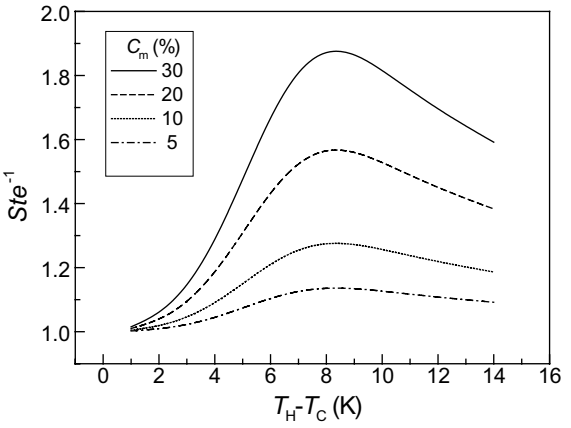

Fig. 19. The reciprocal of modified Stefan number against temperature (The case of $C_m = 30\%$ is from the data measured by DSC, and the others are the calculated by using Eq. (4)).

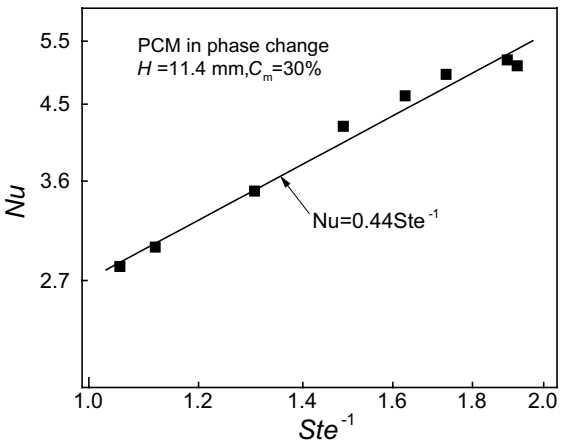

Fig. 20. The relationship between the Nusselt number and the modified Stefan number for the case of $C_m = 10\%$ and AR = 10.5 ($H = 11.4$ mm).

If the hot plate temperature was over the maximum phase changing temperature of $T_H = 323$ K, the Stefan number was given as unity. This means that the effect of phase changing process on natural convection heat transfer can be ignorable. Therefore, in this temperature range the correlation can be simplified as

$$Nu = 0.22(1 - 2.7C_m e^{-0.025AR}) Ra^{1/(3n+1)} \tag{14}$$

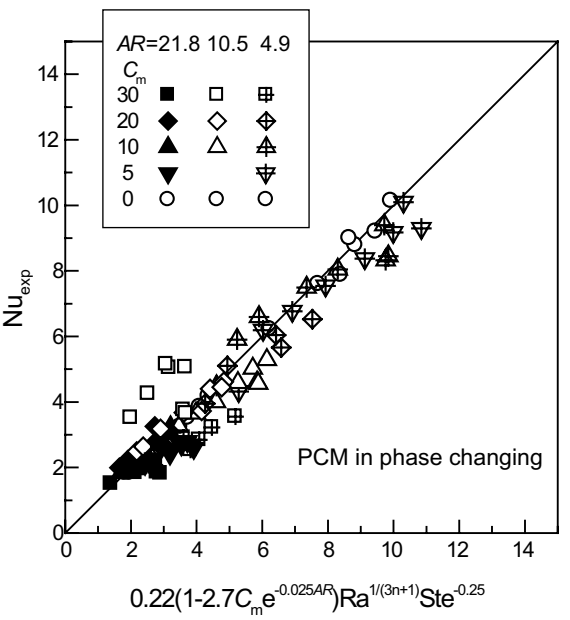

Fig. 21. Comparison of Nusselt number between the experimental data and the correlation Eq. (13) for the PCM in phase changing.

The comparison between Eqs. (11) and (14) shows that all the other coefficients of the two equations are the same except for the effect of aspect ratio. Generally, the side-wall effect of the rectangular enclosure will become significant while the aspect ratio is small, but this also depends upon the viscosity or the Prandtl number of the fluid in the enclosure.

4.3. The PCM in liquid phase

The experimental data were correlated in the same way for the PCM in the liquid phase as in the solid phase. All the phase change material in the microemulsion slurry was in a liquid phase at temperature over 323 K. As shown in Figs. 3–5, the rheological and thermophysical properties are to a lesser extent dependent upon temperature in the range of 323–333 K. However, it should be noted that the volumetric expansion coefficient β in this range is smaller than that of distilled water. Especially at a temperature of 327 K, the volumetric expansion coefficient β reaches its minimum and it is about three times smaller than that of distilled water for the case of $C_m = 30\%$. Since the volumetric expansion coefficient β is small in the liquid phase, the integral averaged method becomes more important to estimate Nusselt number in dependence on Rayleigh number in order to have a physically meaningful result. It is concluded that since the viscosity of the PCM slurry in a liquid phase is less than that in a solid phase, the side-wall effect of enclosure on natural convection heat transfer is also reduced. By using the same method, the best correlation obtained is,

$$Nu = 0.22(1 - 2.0C_m e^{-0.02AR})Ra^{1/(3n+1)} \quad (15)$$

As shown in Fig. 22, the standard deviation of the correlation equation is about ±12% against the experimental data.

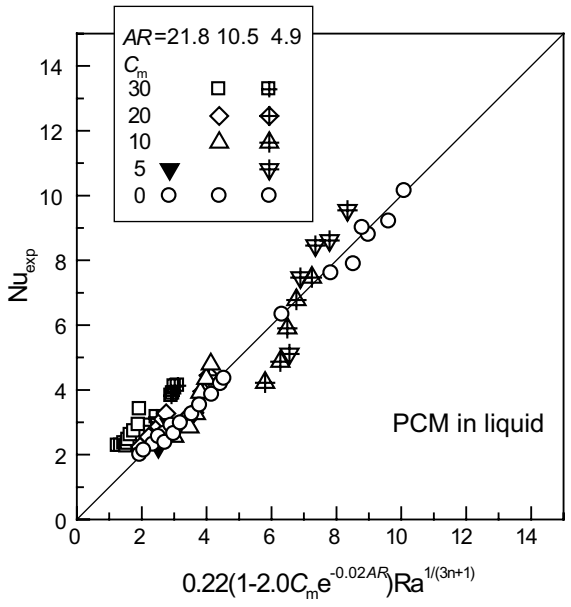

Fig. 22. Comparison of Nusselt number between the experimental data and the correlation Eq. (15) for the PCM in liquid phase.

5. Conclusions

The microemulsion PCM slurry showed very complex natural convection heat transfer characteristics in a horizontal microemulsion PCM slurry layer heated from below and cooled from above. Both effects of the aspect ratio of a rectangular enclosure and the PCM concentration of the slurry on natural convection heat transfer were clarified. Based on the experimental results and the correlated equations, the following conclusions could be drawn.

(1) Even for the lowest PCM concentration of the slurry, the maximum Nusselt number was observed in the phase changing region with an increase in Rayleigh number. The dispersed PCM particles in a microemulsion slurry could enhance the natural convection due to contribution of latent heat generation by melting and solidification. The modified Stefan number was introduced in the present study, which represented the enhancement of natural convection heat transfer resulted from the participation of latent heat with phase change.

(2) The Nusselt number in the phase changing process in the PCM slurry was in proportional to the reciprocal of the modified Stefan number with an exponent of a quarter. The Nusselt number increased with increasing the PCM concentration. However, since the viscosity of the PCM slurry could increase also with an increase in the PCM concentration, the overall heat transfer coefficient decreased with increasing the PCM concentration. This result was in definitely agreement with those obtained by Datta et al. [8].

(3) The side-wall effect of the rectangular enclosure on natural convection heat transfer was greater for the PCM in the solid phase as compared with those in the phase changing and liquid phase because the viscosity of the PCM slurry was decreased by melting the PCM. On the other hand, the side-wall effect on the natural convection heat transfer decreased with a decrease in the PCM concentration. In addition to the viscosity, other physical properties of the PCM slurry varied dramatically in the phase changing process. Therefore, the correlations of Nusselt number obtained of the PCM slurry in a phase

change and liquid phase had a greater deviation than that of the PCM slurry in a solid phase.

References

[1] H. Inaba, S. Morita, Flow and cold heat-storage characteristics of phase-change emulsion in a coiled double-tube heat exchanger, ASME J. Heat Transfer 117 (1995) 440–446.

[2] H. Inaba, New challenge in advanced thermal energy transportation using functionally thermal fluids, Int. J. Thermal Sci. 39 (2000) 991–1003.

[3] P. Charunyakorn, S. Sengupta, S.K. Roy, Forced convection heat transfer in microcapsulated phase change material slurries: flow in circular ducts, Int. J. Heat Mass Transfer 34 (1991) 819–833.

[4] E. Choi, Y. Cho, H.G. Lorsch, Forced convection heat transfer with phase-change-material slurries: turbulent flow in a circular tube, Int. J. Heat Mass Transfer 37 (1994) 207–215.

[5] H. Inaba, M.J. Kim, A. Horibe, Melting heat transfer characteristics of latent heat microcapsule-water mixed slurry flowing in a pipe with constant wall heat flux (experimental study), JSRAE 19 (1) (2002) 13–22.

[6] P. Datta, S. Sengupta, S.K. Roy, Natural convection heat transfer in an enclosure with suspensions of microcapsulated phase change materials, ASME General Papers in Heat Transfer HTD 204 (1992) 133–1446.

[7] L. Katz, Natural convection heat transfer with fluids using particles while undergoing phase change, PhD Dissertation, Department of Mechanical Engineering; Massachusetts Institute of Technology, Massachusetts, 1968.

[8] P. Datta, S. Sengupta, T. Singh, Rayleigh and Prandtl number effects in natural convection in enclosures with microencapsulated phase change materials slurries, Symposium on 33rd Heat Transfer in Japan, 1996, pp. 225–226.

[9] JSME data book: Thermophysical properties of fluids, JSME, 1983.

[10] K.G.T. Hollands, G.D. Raithby, L. Konicek, Correlation equation for free convection heat transfer in horizontal layers of air and water, Int. J. Heat Mass Transfer 18 (1975) 879–884.

[11] V.S. Arpaci, S.H. Kao, Foundations of buoyancy driven heat transfer correlations, ASME J. Heat Transfer 123 (2001) 1181–1184.

[12] S. Ostrach, Natural convection in enclosures, ASME J. Heat Transfer 110 (1988) 1175–1190.

[13] A.V. Getling, Rayleigh–Bénard convection: structures and dynamics, Advanced Series in Nonlinear Dynamics, vol. 11, World Scientific, Singapore, 1998.

[14] H. Ozoe, S.W. Churchill, Hydrodynamic stability and natural convection in Ostwald-de Waele and Ellis fluids: the development of a numerical solution, AIChE J. 18 (6) (1972) 1196–1206.

[15] U. Christensen, Convection in a variable-viscosity fluid: Newtonian versus power-law rheology, Earth Planetary Sci. Lett. 64 (1983) 153–162.

[16] C. Dumoulin, M.P. Doin, L. Fleitout, Heat transport in stagnant lid convection with temperature- and pressure-dependent Newtonian or non-Newtonian rheology, J. Geophys. Res. 104 (B6) (1999) 12759–12777.

[17] E.M. Parmentier, A study of thermal convection in non-Newtonian fluids, J. Fluid Mech. 84 (1978) 1–11.

[18] J.D. Dale, A.F. Emery, The free convection of heat from a vertical plate to several non-Newtonian ''pseudoplastic fluid'', ASME J. Heat Transfer 94 (1972) 64–72.

[19] I.G. Reilly, C. Tien, M. Adelman, Experimental study of natural convection heat transfer from a vertical plate in non-Newtonian fluid, Can. J. Chem. Eng. 43 (1965) 157–160.

[20] H. Inaba, C. Dai, A. Horibe, Numerical simulation of Rayleigh–Bénard convection in non-Newtonian phase-change-material slurries, Int. J. Thermal Sci. 42 (2003) 471–480.